

AD-A063 085

TECHNION - ISRAEL INST OF TECH HAIFA DEPT OF MATERIA--ETC F/G 11/6  
MICROSTRUCTURAL CHANGES FOLLOWING DEFORMATION OF TI-6AL-4V.(U)  
OCT 78 A ROSEN

UNCLASSIFIED

EOARD-TR-78-4

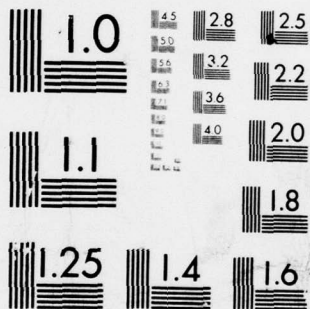
AFOSR-77-3441

NL

OF  
AD  
A063 085



END  
DATE  
FILMED  
3--79  
DDC



MICROCOPY RESOLUTION TEST CHART  
NATIONAL BUREAU OF STANDARDS-1963-A

**LEVEL**

*(Handwritten signature)*

Grant Number AFOSR - 77 - 3441

AD A063085

Microstructural Changes Following Superplastic  
Deformation of Ti-6Al-4V

Abraham Rosen

Department of Materials Engineering  
Technion - Israel Institute of Technology  
Haifa, Israel

25 Oct. 1978

DDC  
RECEIVED  
JAN 9 1979  
F

Final Scientific Report, 15 Sept. 77 - 14 Sept. 78

Approved for public release; distribution unlimited

Prepared for

European Office of Aerospace Research and  
Development, London, England

79 01 08 074

DDC FILE COPY

REPORT DOCUMENTATION PAGE		READ INSTRUCTIONS BEFORE COMPLETING FORM
1. Report Number <u>18</u> <u>EDARD TR-78-4</u>	2. Govt Accession No.	3. Recipient's Catalog Number
4. Title (and Subtitle) <u>MICROSTRUCTURAL CHANGES FOLLOWING DEFORMATION OF Ti-6Al-4V</u>	5. Type of Report & Period Covered <u>9</u> Final Scientific Report. 15 Sept 1977 - 14 Sept 1978	6. Performing Org. Report Number <u>14</u> 048-218
7. Author(s) <u>10</u> Abraham Rosen	8. Contract or Grant Number <u>15</u> AFOSR-77-3441 <i>new</i>	9. Performing Organization Name and Address Department of Materials Engineering Technion - Israel Inst. of Tech. Haifa, Israel
10. Program Element, Project, Task Area & Work Unit Numbers	11. Controlling Office Name and Address	12. Report Date <u>11</u> 25 Oct. 1978
13. Number of Pages	14. Monitoring Agency Name and Address	15. <u>12</u> <u>14</u> p.
16. & 17. Distribution Statement Approved for public release; distribution unlimited.		
18. Supplementary Notes Prepared in cooperation with T. Livin and E. Ganin		
19. Key Words Creep, Superplasticity, Titanium alloys		
20. Abstract Creep tests have been performed in the range 800-900°C on thin specimens of commercially pure titanium. It was observed that, in the temperature range of interest, the mode of failure was strongly dependent upon the imposed creep rate. Transmission electron microscopy revealed that recrystallization occurred during high creep rate deformation and that the recrystallization nuclei often occurred at grain boundary triple points where the dislocation density was relatively high. By contrast in low creep rate experiments there was no evidence of large scale recrystallization or grain boundary migration but dislocation climb appeared to be an important factor in creep in this region. ←		

FORM 1473

445342

7B

This report has been reviewed by the Information Office (EOARD/CMI) and is releasable to the National Technical Information Service (NTIS). At NTIS it will be releasable to the general public, including foreign nations.

This technical report has been reviewed and is approved for publication.

John T. Milton

JOHN T. MILTON  
Scientific and Technical Information  
Officer

FOR THE COMMANDER

Michael A. Greenfield

MICHAEL A. GREENFIELD, Ph.D.  
Deputy Director

Gordon L. Hermann

GORDON L. HERMANN, Lt Colonel, USAF  
Materials Liaison Officer

White Section	<input checked="" type="checkbox"/>
Buff Section	<input type="checkbox"/>
UNCLASSIFIED	
CLASSIFICATION	
UNCLASSIFICATION/AVAILABILITY CODES	
-1/ or SPECIAL	
A	



## Superplastic Deformation of Titanium Alloys

The first report dealt with the building of the special creep apparatus, instrumentation and specimen preparation, while this report deals with creep performed on commercially pure titanium. The reasons for using commercial titanium before investigating the Ti-6Al-4V alloy were twofold: (i) specimen preparation is much easier and (ii) the structure to be studied is much simpler. Since there is no phase change on cooling from the testing temperature, we thought it would be easier to gain "experience" with this relatively simple alloy before going on to study the more complicated two-phase Ti-6-4.

Our intention was to study by means of transmission electron microscopy the effect of temperature, creep rate and creep strain on the structure and compare it with the structure of uncrept specimens which have been exposed to the same thermal history.

All the specimens were prepared from a single 0.8 mm thick titanium sheet by rolling to a thickness of 0.3 mm without intermediate annealing. Specimens 3 mm wide and 6 mm gauge length were machined parallel to the rolling direction. The specimens were recrystallized at 700°C for 4 minutes in vacuum. The average grain size after recrystallization was approximately 10  $\mu\text{m}$ .

A typical creep experiment was conducted as follows: Two very thin chromel-alumel thermocouples were spot-welded to the specimen at both ends of the gauge section with a distance of 6 mm between the two. The spot-welding was done very carefully so as not to damage the metal. The specimen was gripped and the small furnace was located such that the center of the specimen coincided with the center of the furnace. Another specimen was also located in the furnace which was, however, not connected to the loading device. A pre-set load was chosen but was not yet applied.

79 01 08 074

After setting the LVDT to a starting position, the vacuum jar was set in place and when a vacuum of  $3-6 \times 10^{-5}$  mm Hg was reached, the furnace power was switched on. It took just a few minutes to reach the desired temperature (about  $800^{\circ}\text{C}$ ). If the two thermocouples showed slightly different temperatures, the furnace was moved up or down with the help of a screw outside the vacuum jar until both thermocouple readings were exactly the same. Upon reaching the constant temperature, the load was released and the creep experiment begun. The strain was continuously recorded with a standard x-t recorder. Creep tests were run between 5-60 min. depending on the initial creep stress. Immediately after fracture, pure argon gas was released on the specimen which cooled down in a matter of seconds to about  $500^{\circ}\text{C}$ .

A typical creep curve is shown in fig.1. It is to be noted that this is a constant-load curve and the stress changes, first linearly with elongation when the deformation is uniform, and then very rapidly when necking begins. There is also a few degrees change in temperature, measured by the lower thermocouple since the lower part of the specimen moves out of the hot zone of the furnace.

Table 1 summarises the results of some of the creep experiments i.e. initial temperature, creep stress, initial creep rate, time of rupture and total elongation.

Fig.2 shows the photograph of two specimens which were creep tested. Both crept at the same temperature,  $850^{\circ}\text{C}$ . The initial stress on specimen (a) was  $11.5 \times 10^{-6} \text{ N/m}^2$ , and on specimen (b) was  $8.6 \times 10^{-6} \text{ N/m}^2$ . The corresponding initial strain rates were  $1.7 \times 10^{-4}$  and  $1.56 \times 10^{-5} \text{ sec}^{-1}$  respectively. Total elongation was 115% for specimen (a) and 67% for specimen (b). It is clearly seen in fig.2 that specimen (a) has a long diffused neck, while specimen (b) has a more localised neck. Diffused necking is a superplastic feature and inspite of the fact that total elongation

was only 135%, probably due to the use of very small specimens to begin with. We can assume that specimen (a) deforms "more superplastically" than specimen b. All specimens creep tested under large stress which resulted in a relatively high strain rate, deformed similarly to specimen (a), while those tested under smaller stress deformed like specimen b.

Specimens for transmission electron microscopy were prepared as 3 mm diameter discs which were subsequently jetted and electro polished in standard solutions. All specimens were examined in a 100 kV TEM.

Fig.3 shows the microstructure of a non-crept specimen which was held at 802°C for 39 minutes. The general feature is large equilibrium shaped grains with very few dislocations. Very little, probably less than 2%  $\beta$ , is located at grain boundary triple points (see fig.4) possibly arising from iron impurities. Figs.3 and 4 exhibit the typical microstructure of all non-deformed specimens.

Figs.5 to 8 show the microstructure of a specimen which was creep tested at 802°C under a stress of  $11.4 \times 10^{-6} \text{ N/m}^2$ . This specimen was treated together with the one shown in figs.3 and 4. It was an "a type" specimen with a long diffused neck. Fig.5 shows how the dislocation free grains (shown in figs.3 and 4) become densely populated by dislocations, forming subgrain boundaries. Fig.6 shows a dislocation free new recrystallised grain at the junction of deformed grains. Figs.7 shows inward curved grain boundaries about to annihilate a heavily deformed old grain. Some of the recrystallised grains also contain dislocations which were probably created by continuous deformation. Fig.8 exhibits the elimination of an elongated grain by its neighbours. The right hand grain which was recently recrystallized, had begun to deform again growing out towards the left hand side. The left hand grains probably also recrystallized and newly deformed during creep.



The following micrographs, figs 9-11, were taken from a specimen which had been creep tested at  $840^{\circ}\text{C}$  under the same stress as the former one. It also had an "a type" neck. The structure is very similar to that shown before, except that there is a little more transformed  $\beta$ . Fig.9 shows a former  $\beta$  grain which transformed on cooling to  $\alpha$  and  $\beta$ . A dislocation source is seen to be operating from an  $\alpha$  -  $\beta$  grain boundary. Some of the  $\alpha$  grains are dislocation free due to recent recrystallisation. Fig.10 is an example of low angle boundary sub-grain formation with very high dislocation density and non-equilibrium grain shape. Fig.11 shows a grain boundary migrating into a region of very high dislocation density. The lower part of the same grain moves more slowly since the dislocation density is much lower there. All dislocations are heavily jogged by interaction with each other. Dislocation generation is apparently heavier at grain corners.

The following two micrographs, figs. 12 and 13, are taken from a specimen which was deformed at  $840^{\circ}\text{C}$  under a creep stress of  $8.6 \times 10^{-6} \text{ N/m}^2$ , which resulted in a rather low creep rate. This specimen deformed by a "b type" localized neck. The general appearance of the microstructure, as shown in fig. 12, is quite similar to that of the "a type" specimens, except that there is less tendency to subgrain formation and less evidence of recrystallisation. A completely new feature which is not seen in "a type" specimens is shown in fig.13. The figure shows a high concentration of jogged dislocations (with climb loops at the intersections).

Although it would be too early at this stage of the investigation to draw conclusions, the results presented in this report strongly suggest that commercial titanium creep tested between  $800$ - $860^{\circ}\text{C}$  deforms super-plastically under certain conditions. The TEM study indicates that when the applied stress is large and the corresponding initial creep rate is high, a considerable amount of elongation can be accommodated by the following

mechanism: Dislocations are created during creep. Favorable multiplication sites are grain boundary triple points or  $\alpha - \beta$  interfaces (see fig.9). The dislocations interact and the initially large grains are divided into subgrains (fig.5). The interior of these subgrains is densely populated by dislocations (fig.10). Since the creep rate is high, the rate of dislocation multiplication is higher than the rate of annihilation by thermally activated processes, such as climb. When the amount of plastic deformation reaches a critical value, recrystallization sets in, creating new dislocation free grains (fig.6). These grains then grow into heavily deformed grains (fig.11) and the total dislocation density decreases. With continuous creep the newly formed grains are being deformed again and the sequence of subgrain formation and dynamic recrystallization is going on. Due to dynamic recrystallization, strain hardening should be minimal and deformation gives rise to a long diffused neck. The suggested deformation mechanism is similar to the phenomenon of transformation plasticity, but in this instance, recrystallization occurs instead of phase transformation.

When the applied stress is small and the corresponding creep rate is low, dislocation climb is a more effective annihilation process (see fig.13). Deformation induced dislocation density is lower, subgrain formation and subsequent recrystallization is less evident and the specimen deforms uniformly by normal creep processes until the appearance of a neck followed by fracture.

TABLE 1

$T^{\circ}\text{C}$	$\sigma \text{ N/M}^2 \times 10^{-6}$	$\dot{\epsilon} \text{ sec}^{-1} \times 10^{-4}$	t min	$\epsilon\%$	type
802	11.42	0.35	39.0	110	a
820	11.46	0.92	19.7	133	a
840	11.46	1.70	17.5	113	a
840	8.62	0.156	81.0	67	b
849	15.98	14.6	3.0	135	a
851	16.55	21.1	2.0	118	a
865	11.68	1.87	3.3	107	a
891	8.43	2.6	17.0	80	b

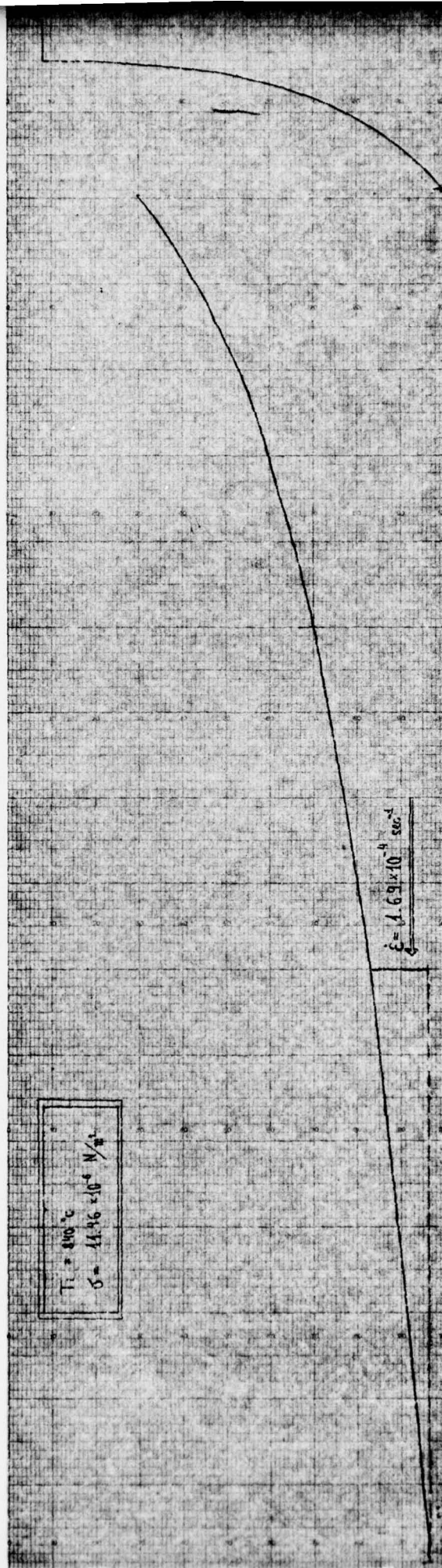


FIG. 1



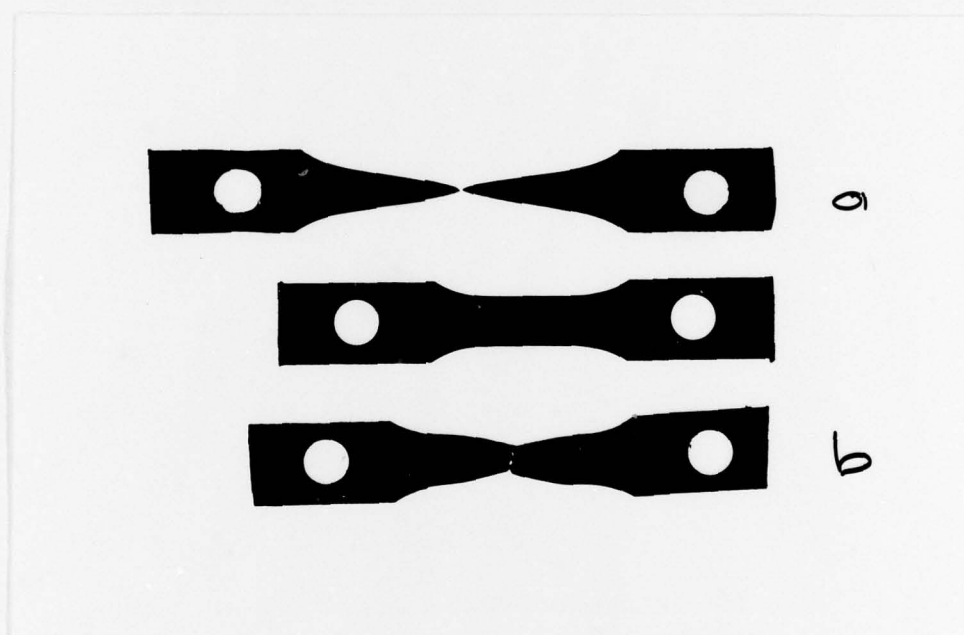


FIG. 2



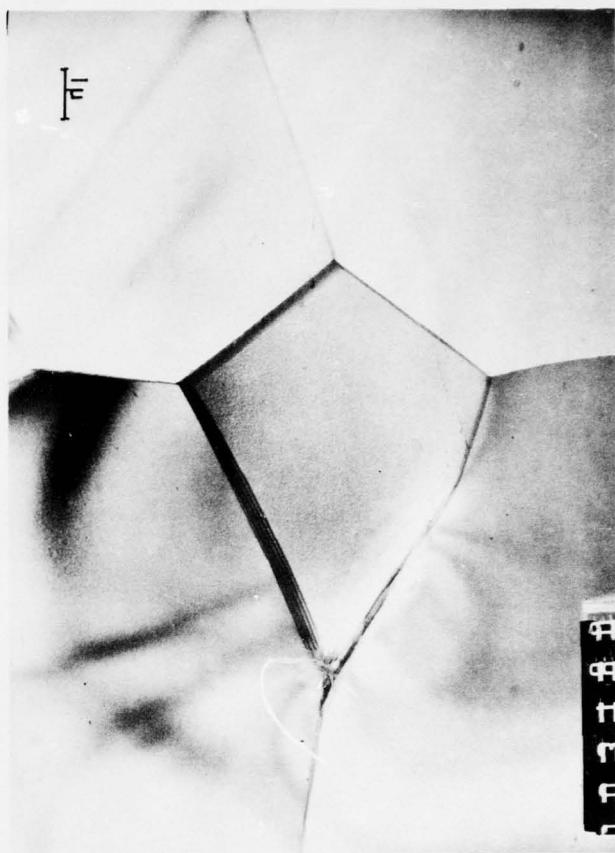


FIG. 3



FIG. 4



FIG. 5



FIG. 6



FIG. 7

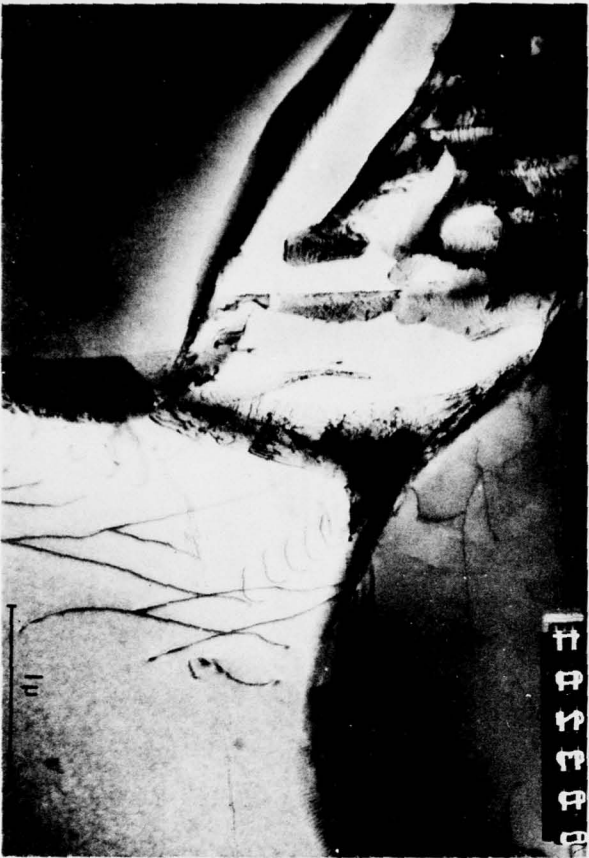


FIG. 9



FIG. 8



FIG. 10



FIG. 11

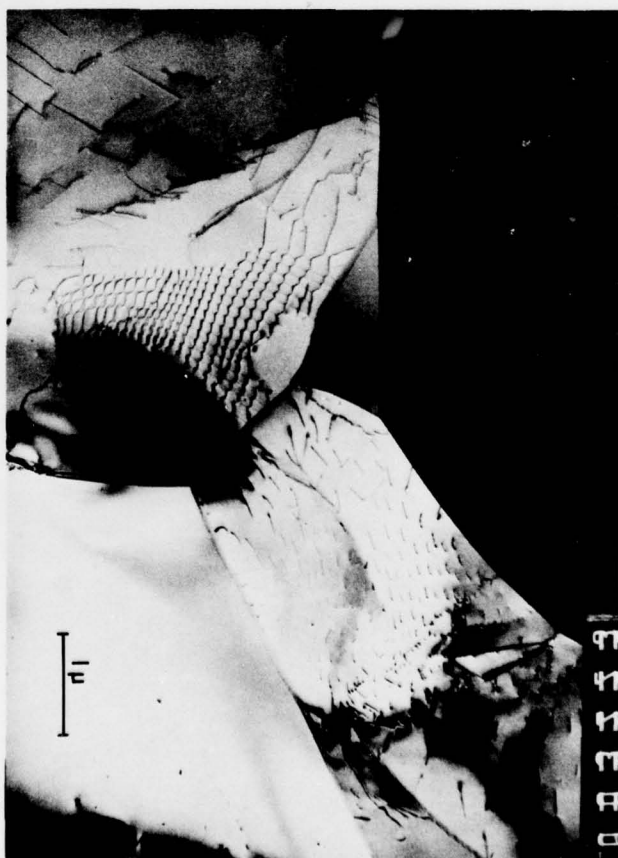


FIG. 12

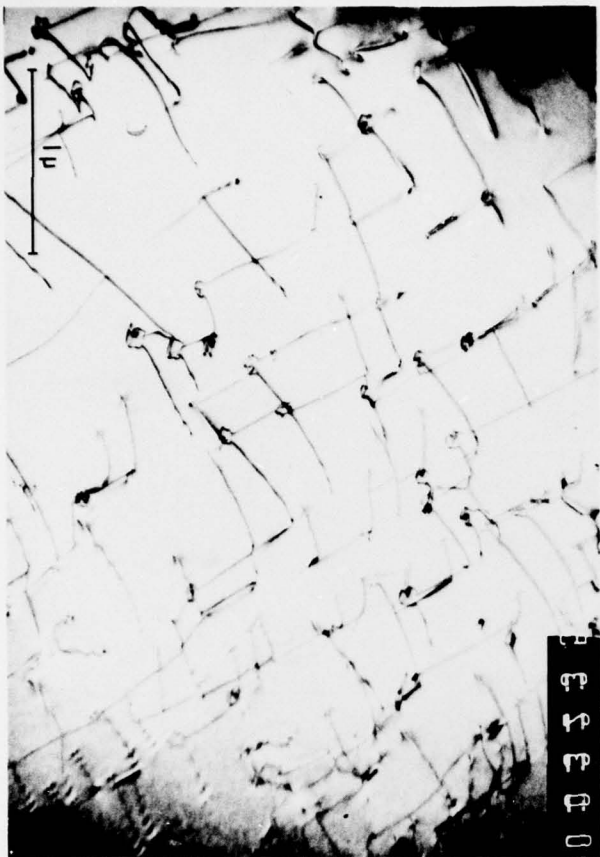


FIG. 13